Available online at www.sciencedirect.com
SCIENCE DIRECT®
Journal of Nuclear Materials 337–339 (2005) 839–846
journal of nuclear materials
www.elsevier.com/locate/jnucmat

Redeposition of hydrocarbon layers in fusion devices

Wolfgang Jacob *

Centre for Interdisciplinary Plasma Science, Max-Planck-Institut für Plasmaphysik, Abt. OP, Geb. D3, Postfach 1533, EURATOM Association, Boltzmannstr. 2, D-85748 Garching, Germany

Abstract

Co-deposition of hydrogen isotopes with carbon in nuclear fusion experiments is a topic of paramount importance for a next-step device. Physical sputtering, chemical erosion, and chemical sputtering of carbon by hydrogen isotopes lead to release of hydrocarbon species which are transported to plasma shaded regions and lead there to deposition of co-deposited layers. Co-deposition is generally believed to be the dominant tritium retention mechanism in a next-step device. The article reviews recent experimental results regarding co-deposition in fusion devices, and basic low-temperature plasma and particle-beam experiments relevant to co-deposition of hydrocarbon layers in nuclear fusion devices.

PACS: 52.40.Hf; 68.55.Jk; 81.15.Gh; 82.65.+r
Keywords: Amorphous films; Chemical erosion; Co-deposition; Deuterium inventory; Erosion and deposition; Hydrocarbons; Hydrogen inventory; Sputtering; Surface analysis; Thermal desorption; Tritium

1. Introduction

One of the most crucial plasma–wall-interaction issues for a next-step device such as ITER is tritium retention via tritium co-deposition with eroded carbon. This is expected to be the dominant tritium retention mechanism [1]. In most existing fusion experiments the divertor surface consists of graphite tiles or carbon fiber composites which are exposed to a substantial incoming flux of ions and neutrals from the main plasma. This impinging species flux leads to erosion of the divertor tiles emitting carbon and hydrocarbon compounds into the gas phase. Most of the carbon and hydrocarbon species released in the divertor will redeposit in relative close proximity to their place of origin. This balance between deposition and erosion is crucial for the performance of a divertor in a next-step device, since the total lifetime before replacement strongly depends on the ability to control this redeposition. However, the small fraction of carbon and hydrocarbon species that is not redeposited in the divertor may escape from the divertor and also from the boundary plasma and cause deposition of hydrocarbon layers – often called *redeposited* or *co-deposited* layers – on surfaces not in direct contact with the plasma. Indeed, thick redeposited layers were observed on remote surfaces of JET [2]. More recent investigations resulted in the detection of much thinner, but measurable, redeposited layers in other tokamaks (e.g., TEXTOR [3] and ASDEX Upgrade [4–8]). On many of these surfaces only neutral carbon-carrying growth precursors can contribute to film deposition, because only they can traverse the magnetic field lines. A major concern is the large amount of hydrogen isotopes trapped in these redeposited films [1] because in a future fusion reactor

* Tel.: +49 89 3299 2618; fax: +49 89 3299 1149.
E-mail address: wolfgang.jacob@ipp.mpg.de

0022-3115/$ - see front matter © 2004 Published by Elsevier B.V.
doi:10.1016/j.jnucmat.2004.10.035

this trapped hydrogen will partly be tritium. One aim of a future design is, therefore, to reduce this tritium retention for economy and safety reasons.

2. Co-deposited layers in fusion devices

Plasma–material interactions in current tokamaks were comprehensively reviewed in 2001 by Federici et al. [1] and the hydrogen inventories in nuclear fusion devices have been reviewed by Mayer et al. [3]. In this section, more recent results of the analysis of co-deposited carbon layers in nuclear fusion experiments will be briefly summarized. Thereby, the main emphasis will be put on the following questions: Where does the main deposition occur? What are the species leading to deposition? And, how can we explain the observed deposition patterns?

Thick co-deposits of up to 90 μm thickness were found at the inner wall of the divertor tiles of JET following the experimental period from 1999 to 2001 [9]. In general, the inner divertor is deposition dominated while the outer divertor is a net erosion area [2,9]. Ion beam analysis and secondary ion mass spectroscopy (SIMS) of deposited layers on the inner JET divertor tiles which have plasma contact indicate that C is probably eroded from these deposits, leaving behind films rich in Be and other metals [2,9]. In adjacent regions shadowed from direct plasma contact thick carbon deposits with high D content (up to D/C = 0.8), but no beryllium, are found [2,10,11]. In addition, thick co-deposits substantially contributing to the fuel inventory in the torus were found in tile gaps [8]. It is further interesting to note that the deposition/erosion behavior of carbon in JET significantly changed when the wall temperature was reduced in 2001 [9]. For the last three months of operation prior to the 2001 shutdown, the vessel wall temperature was reduced to 470 K from the normally used 590 K and it appears that this significantly reduced the removal of carbon by chemical erosion. In addition, investigations applying cavity substrates [12–14] led to the conclusion that a large fraction of high sticking species contributes to the deposition in the JET divertor [11].

A rather comprehensive investigation of carbon deposition and erosion on ASDEX Upgrade divertor tiles was performed for the experimental campaign 2002/2003 [7]. It was found that the inner divertor is a net carbon deposition area while the outer divertor is erosion dominated. Deposition is maximal at the inner strike point positions (up to 6 μm thick layers), but there also exist areas with high deposition where the strike point was never positioned. The deuterium content in the layer shows large variations and appears to be mostly influenced by the temperature history of the tiles. In areas not in direct line of sight to the plasma deuterium rich layers with D/C up to 1 are observed. In contrast to JET, where most carbon is found under the divertor, e.g., on the louvers, most of the carbon deposition is on the divertor tiles. In ASDEX Upgrade only about 10% of the deposited carbon is found under the divertor structure [7]. These deposits in remote areas are soft hydrocarbon layers with high D content [6,15]. As in JET, investigations applying cavity substrates indicate that the deposition under the divertor is dominated by high sticking species [16]. The same conclusion is drawn by Rohde et al. [15] who analyzed long term samples exposed under the divertor during the last campaign in ASDEX Upgrade. In addition, they found large asymmetries in the deposition pattern on samples exposed at comparable locations, but facing different directions. Although the occurrence of a parasitic plasma [4] underneath the divertor complicates the interpretation of the data, it appears that these asymmetries can only be explained by erosion processes.

In TEXTOR-94 hydrogen-rich co-deposited layers with thicknesses of up to 1 mm have been found on recessed parts of the limiters [3]. On the ALT-II limiter thick deposited layers (up to 50 μm) were found in the net deposition areas. This is particularly remarkable because most of the limiter area is erosion dominated. These layers posses a relatively low D content which can be attributed to temperature excursions, e.g., during disruptions or long pulse discharges [2]. The deposited layers contain hydrogen isotopes of up to (H + D)/C = 0.4. Layers deposited far away from the plasma, e.g., in the pump ducts show H isotope contents of up to (H + D)/C ≈ 2; their contribution to the total inventory remains, however, low, i.e., of the order of a few percent [17].

In addition to these postmortem analyses of tokamak tiles and long term samples, investigations with quartz microbalances (QMB) in JET [18] and ASDEX Upgrade [15] provide time-resolved measurements on a shot-to-shot basis. These investigations revealed that the growth of redeposited layers on the QMB's is a continuous process. The growth rate varies depending on the plasma scenario; the growth rate is particularly high if the QMB is in line of sight to the main particle source, i.e., the inner divertor strike point.

3. Investigations using low-temperature laboratory plasmas

Experiments applying low-temperature laboratory plasmas for investigation of deposition and erosion in the hydrogen–carbon system can be separated in two groups: (i) plasma simulators and (ii) small scale standard low-temperature plasmas (LTP). The first group consists of two major experimental efforts, the PISCES facility at the University of San Diego [19] and PSI-2

now at the Humbold University, Berlin [20,21]. These two experiments are dedicated to the investigation of plasma–surface-interaction (PSI) processes relevant for nuclear fusion plasmas. They provide very valuable information about PSI processes in parameter ranges relevant for ITER. The second group of experiments spans a huge range of very different groups and setups. Most of them are dedicated to the deposition of a–C:H layers for technological applications. Here I will limit the discussion to small-scale laboratory LTP experiments relevant to co-deposited layers in fusion devices. The primary source for hydrocarbon species that lead to co-deposition in fusion devices is erosion of carbon surfaces through interaction with a hydrogen plasma. Therefore it is also necessary to have a closer look to the erosion processes in this system.

The temperature dependence of the deposition of a–C:H films was investigated by von Keudell and Jacob [22]. Deposition was performed in an electron cyclotron resonance (ECR) plasma using methane as working gas. Erosion and deposition was measured using in situ, real-time ellipsometry. With increasing temperature the deposition rate decreases and for temperatures greater than 500 K erosion occurs; see Fig. 1. The temperature dependence of the erosion rate is also shown in Fig. 1. It is clearly evident from Fig. 1 that the temperature dependence is the same in both processes. The conclusion from this experiment is that the temperature dependence observed for deposition of a–C:H layers is given by the temperature dependence of the erosion process. Responsible for the erosion is the copiously available hydrogen in the plasma which is produced by electron-induced dissociation of the working gas [23]. The net deposition is the difference of a temperature-independent deposition process and a temperature-dependent erosion process. Increasing the substrate temperature under constant particle fluxes enhances the erosion efficiency and the net deposition decreases. This can also explain the change-over from net deposition to net erosion shown in Fig. 1. It is clear that the change-over temperature for this effect depends on the relative fluxes of deposition and erosion species.

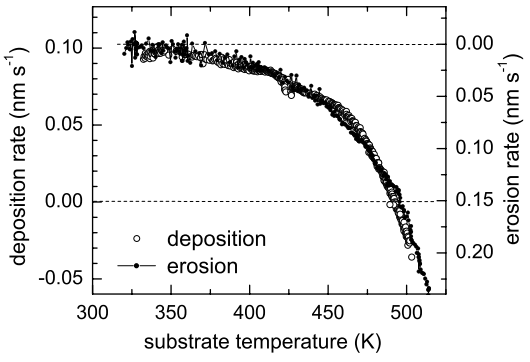

Fig. 1. Comparison of the deposition and erosion rates of a–C:H films in methane and hydrogen low-temperature plasmas, respectively, as a function of temperature [22]. Deposition and erosion were measured by real-time ellipsometry with the substrate at floating potential which corresponds to ion energies of about 15 eV. The left-hand scale is for the deposition and the right-hand scale for the erosion experiment. Note the different scales, especially the shift in the zero position for the two cases.

It is well known that the structure and physical properties of a–C:H layers depend sensitively on the deposition conditions [23]. The most important deposition parameter is the energy of ions impinging on the growing film surface during deposition [23,24]. At low ion energies (<50 eV), soft, polymer-like layers with high hydrogen content grow, while at high ion energies (>50 eV), hard, amorphous layers with a hydrogen content of typically H/C $\approx$ 0.4 are deposited. The erosion rates for different a–C:H layers differ significantly [22,25,26]. The actual erosion rate for a specific a–C:H layer depends, however, not only on its bulk properties, but also on the actual dynamic state of the surface during interaction with the plasma [22,23]. This is demonstrated in Figs. 2 and 3, where the erosion rates are shown for soft and hard a–C:H layers, respectively, as a function of temperature.

In Fig. 2 the erosion rate of soft a–C:H layers is plotted as a function of temperature at floating potential (solid line) and with an additional substrate bias of −100 V [22]. Erosion was measured in an ECR hydrogen plasma using real-time ellipsometry. The erosion rate at floating potential is negligible for low temperature (<350 K), but increases exponentially with increasing

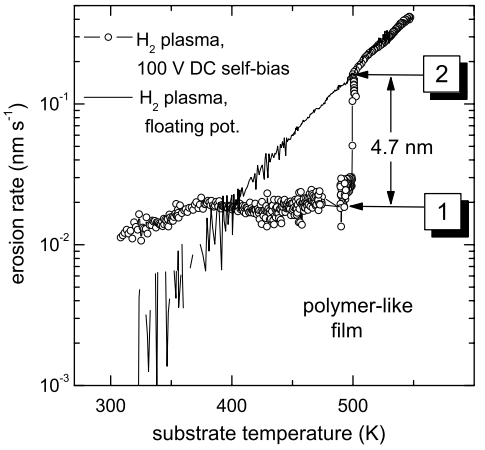

Fig. 2. Erosion rate of a soft a–C:H layer as a function of temperature at floating potential (solid line) and with an additional substrate bias of 100 V. Erosion was measured in an ECR hydrogen plasma using real-time ellipsometry [22]. At point 1 the bias voltage was switched off. At point 2 the same rate as for the run without bias is measured. The eroded layer thickness between points 1 and 2 is 4.7 nm.

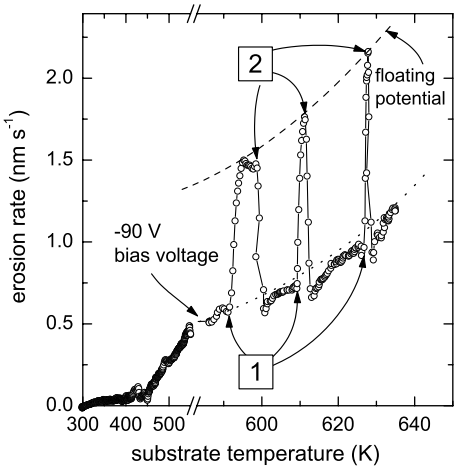

Fig. 3. Erosion rate of a hard a–C:H layer as a function of temperature. Erosion was measured in an ECR hydrogen plasma using real-time ellipsometry [22]. The additional bias voltage during deposition and erosion of this layer was 90 V. At higher temperatures the additional substrate bias was switched off (points 1) and on (points 2). The erosion rate jumps between the two curves indicated by the dashed and dotted lines.

temperature. If an identical layer is eroded with an additional substrate bias voltage of −100 V, the rate at low temperature is, as anticipated, significantly higher than without bias. But the increase of the erosion rate with increasing temperature is negligible, compared with the case without bias. In fact for temperatures higher than about 400 K the rate with bias is even lower than the rate without bias. At point 1 in Fig. 2 (≈500 K) the bias voltage was switched off. After a short delay, the erosion rate increases and at point 2 the same erosion rate is reached as for the run without bias. The eroded layer thickness between points 1 and 2 is 4.7 nm. The interpretation is as follows: the increase of the erosion rate with increasing temperature for the case without bias is due to the well known temperature dependence of chemical erosion due to atomic H [26,27] which is abundant in these types of plasmas. A requirement for thermally activated chemical erosion is a high density of chemically bonded H in the surface. This leads to the formation of terminal CH_3 groups which are the precursors for chemical erosion. Ion bombardment of the surface enhances the erosion rate at low temperature where the thermally induced effect is negligible. But at high temperature, ion irradiation reduces the efficacy of chemical erosion because it reduces the H content in the surface, thus destroying the CH_3 groups, the precursor states for chemical erosion [23].

In Fig. 3 the erosion rate of a hard a–C:H layer as a function of temperature is shown. The additional bias voltage during deposition and erosion of this layers was −90 V. At higher temperatures the additional substrate bias was switched off (points 1) and on (points 2) [22]. The erosion rate jumps between the two curves indicated by the dashed lines. But surprisingly, the erosion rate with bias is again smaller than without bias. At these temperature we are close to the maximum of chemical erosion ($T_{max} \approx 650$ K). Interaction of the plasma with the substrate being at floating potential – in this case the ion energy is rather low (≈15 eV) – obviously leads to a state of the surface which is easily eroded. Ion irradiation again destroys this state leading to a surface that is harder to erode. Without bias, H atoms and low-energy ions are chemically incorporated into the surface leading to a hydrogenation of the surface. As discussed above for the soft films, a hydrogenated surface is the precursor for chemical erosion. Again, as above, ion irradiation depletes H from the surface, thus reducing the efficacy of chemical erosion. For more details about these surface effects the reader is referred to Ref. [23]. An important result of these investigations is that the surface is modified due to interaction with the plasma and this modified state of the surface is more determined by the actual plasma–surface-interaction than by the bulk material.

From these various LTP experiments we can draw the following conclusions:

- Different kinds of a–C:H layers have different erosion yields in H plasmas. The higher the H content, the higher is the yield.
- The yield increases with temperature and ion energy.
- The erosion yield depends on the dynamic state of the surface during interaction with the plasma. This can also cause a reduction of the observed yields, e.g., reduction of the erosion rate at high temperature in the erosion with bias voltage as presented in Fig. 2.

Further knowledge collected by LTP experiments is the determination the surface loss probability of hydrocarbon radicals by the cavity technique [13,14]. Cavities with defined geometry were exposed to ECR plasmas using different hydrocarbon gases. Cavities were exposed such that only neutral species and no ions could reach the entrance slit. The surface loss probability β is derived from the deposition profile inside the cavity. β comprises two contributions: the sticking coefficient s and the transformation probability γ, i.e., $\beta = s + \gamma$. The parameter s describes the sticking probability of a species leading to film growth and γ is the probability for a reaction of the species with the surface leading to the formation of a non-sticking species that leaves the surfaces and is lost for further reactions. From their analysis of a variety of different deposition profiles, Hopf et al. [13] concluded that three different β values are sufficient to describe all measured profiles. They suggested that the hybridization of the carbon atom carrying the dangling bond is responsible for the surface loss probability

of a hydrocarbon radical. The following values were determined: $\beta(C_2H) = 0.80 \pm 0.05$ (sp^1 hybridization), $\beta(C_2H_3) = 0.35 \pm 0.15$ (sp^2 hybridization), and $\beta(C_2H_5$ or $CH_3) < 10^{-3}$ (sp^3 hybridization). β represents an upper limit for the sticking coefficient. As a first approximation it can be assumed that $s \approx \beta$, i.e., $\gamma \approx 0$. The most probable anticipated transformation reaction is abstraction of H from the surface leading to the formation of a stable hydrocarbon radical. These reactions are of Eley-Rideal type and posses in general a rather low reaction cross-section. Since these cross-sections are not known for most hydrocarbon radicals, we consider the abstraction of surface-bonded H by atomic H. This reaction was studied by Küppers and co-workers [27] and a reaction probability of the order of 1% was found. The abstraction cross-section for H by impinging CH_3 was determined to be at least one order of magnitude lower [28]. On the other hand, we have to assume that the abstraction probability for radicals with higher reaction probability is also higher. As long as no quantitative measurements for the sticking coefficient of the various hydrocarbon radicals exist, this ambiguity remains. It is, however, reasonable to assume that γ represents only a minor contribution to the total surface loss probability.

LTP experiments significantly enhanced our understanding of growth and erosion of hydrocarbon layers. Although many results are only qualitative, it was possible to determine in some favorable cases quantitative data. One such example is the determination of surface loss probabilities presented above. These results can serve as input parameters for edge simulation codes to assess co-deposition in nuclear fusion devices. A deeper and mostly quantitative understanding of microscopic plasma–surface-interaction processes can be achieved in experiments using quantified particles beams. Results from this approach are presented in the following section.

4. Investigations with particle beams

Plasma–surface-interaction processes in low-temperature plasmas as well as in nuclear fusion devices involve heterogeneous reactions of various radicals and ions, which interact simultaneously with a substrate. Thereby, chemisorption of a specific neutral growth precursor might be enhanced due to surface activation by other incident species. Surface activation depends on identity and energy of incident species, which is illustrated by two examples:

- *Ion-induced chemisorption of neutral radicals*: The kinetic energy of incident ions is dissipated in a collision cascade in the solid. Within this cascade, target atoms are displaced and chemical bonds are broken. If such a broken bond (dangling bond) is created at the physical surface, it might serve as a chemisorption site for incident neutral radicals from the plasma, thus enhancing the sticking probability of impinging species. This process is called *ion-induced chemisorption*.
- *H-atom-induced chemisorption of neutral radicals*: dangling bonds at the physical surface can also be created by chemical reactions [27]. In many low-temperature plasmas, but in particular, in nuclear fusion divertor plasmas, atomic H is an important constituent. The abstraction of surface-bonded H by incident H atoms creates dangling bonds, which then serve as preferred chemisorption sites for incident neutral radicals. This mechanism is called *H-atom-induced chemisorption*.

Due to the complexity of these heterogeneous surface processes, any quantitative prediction of reaction rates based on elementary mechanisms has so far been very limited. A number of such mutual interactions between different types of species has recently been investigated in a particle-beam experiment [29,30]. In addition to the above mentioned processes, the simultaneous interaction of energetic ions and atomic H with carbon surfaces leads to chemical sputtering of the surface; see for example [31–33]. Recent reviews of chemical sputtering include [29,34]. Although no further discussion of chemical sputtering will be presented here, it is important to note that chemical sputtering is the process that causes the erosion of carbon surfaces through the release of hydrocarbon species which in turn are the precursors for redeposition in remote areas.

The sticking coefficient, s, of CH_3 on a hydrocarbon surface was determined to be between 10^{-5} (perpendicular incidence) and 10^{-4} (45° incidence) [28,35,36]. These experimental results are in excellent agreement with molecular dynamics simulations [37,38]. It was further shown that a simultaneous flux of CH_3 and atomic H causes a significant increase of s (*H-atom-induced chemisorption*). The sticking coefficient of CH_3 increases with increasing H flux and saturates for high H fluxes (H/CH_3 flux ratio $\geqslant 100$) at about 10^{-2} [28,35,36].

Similar to surface activation by atomic H, ion-induced dangling-bond formation at the physical surface also provides chemisorption sites for incident radicals from the plasma [39–41]. An ion flux of the order of 10% of the CH_3 flux can increase the sticking coefficient of CH_3 to some 10^{-2}. In this case the net growth rate corresponds to a balance between the rate for ion-induced chemisorption minus the sputtering rate. The incident ion bombardment also causes a change of film stoichiometry. Due to the lower displacement threshold for H compared with carbon [23], bonded H is predominantly displaced within a collision cascade. Displaced H atoms recombine locally forming H_2 molecules, which

diffuse to the surface and desorb [42]. This subsurface H_2 formation leads to a decrease of the H content within the ion penetration range and to cross-linking of the remaining carbon network. Summarizing, one can state that the influence of the ion bombardment on film formation is dominated by two processes, the ion-induced surface activation which influences the deposition rate and the subsurface hydrogen depletion which determines the film properties.

Another set of beam experiments was performed by Zecho et al. [43,44]. They exposed a thin hard a–C:H layer (H/C about 0.4) to a beam of atomic H and measured the erosion products by a line-of-sight mass spectrometer. The dominant erosion products are C_1, C_2, and C_3 hydrocarbons. The erosion yield exhibits a maximum of about 0.01 eroded C per incident H around 750 K. Higher hydrocarbons (C_4 to C_8) were found as minority species. Above 750 K the erosion yield decreases again due to thermally activated dehydrogenation of the layer. Thermal annealing of as-deposited a–C:H layers leads to desorption of H_2 (about 90% of the H is released as H_2) and hydrocarbon products with a similar distribution as seen during chemical erosion of the film [43,44]. In this case only about 1% of the carbon atoms in the layer are removed. Above 900 K, graphitization of the layer sets in. H atoms rapidly rehydrogenate the surface of an annealed a–C:H film at temperatures as high as 800 K. But this process is restricted to a thin surface layer. Chemical erosion of preannealed layers is rather similar to that of as-deposited layers. It should be mentioned here that thermal decomposition of soft layers proceeds significantly differently than that of hard layers. Increasing H content in the soft layers leads to a decrease of the release temperature, a drastic change of the species distribution, and an increase in the total number of released carbon atoms [45]. While for hard layers H_2 is by far the dominating released product, soft layers dominantly release hydrocarbons with large contributions of long chain hydrocarbons. A large fraction of the carbon atoms can thus be mobilized leading in extreme cases to the evaporation of the complete layer.

5. Conclusion

Although the primary source of carbon in the divertor region of tokamaks remains unclear, the transport in the plasma boundary layer seems to cause a migration from the outer divertor along the main chamber wall to the inner divertor. On its way to the inner divertor, carbon is deposited and eroded multiple times. If it comes to rest in a plasma shaded region in the main chamber there is a high probability that it is not reeroded and remains permanently deposited. This leads to film deposition in tile gaps and other plasma shaded regions. Most carbon is, however, transported to the inner divertor leading to thick co-deposits close to the strike point. Depending on the actual plasma conditions (e.g., attached or detached) different kinds of a–C:H layers can form which in turn have different erosion properties. Most of the permanent net deposition occurs in line of sight to the main erosion or recycling areas with steep thickness gradients. But because the depositing species have to cross magnetic field lines, it is evident that most of them have to be neutral species. It is therefore concluded that neutral hydrocarbon radicals are precursors for film growth in remote areas. These hydrocarbon radicals may be produced by electron-induced dissociation of stable molecules released during the chemical sputtering process or be directly produced at the surface. The production of stable molecules has clearly been shown in several experiments [43,44,46–48].

It was further shown that different types of hydrocarbon species have largely different sticking probabilities [13]. The sticking probability depends mostly on the hybridization of the carbon atom carrying the dangling bond. It is very high for sp^1 hybridization, intermediate for sp^2 hybridization, and very low for sp^3 hybridization. Measured and estimated sticking probabilities for a variety of hydrocarbon radicals are summarized in Table 1.

The variety and amount of CH species produced during chemical sputtering depends sensitively on the plasma conditions. It appears that for low ion energies the contribution of higher CH species increases. Also, for intermediate temperatures (≈500 to 700 K), a high contribution of long chain CH species is anticipated. This is, for example, seen in optical spectroscopy of laboratory [49] and divertor plasmas [50,51] through the increase of the C_2 band and was demonstrated in the laboratory experiments by Zecho et al. [43,44]. Based on this observation we may hypothesize that the huge deposition seen in JET louvers occurred because JET was operating at that time in a plasma regime (wall temperature about

Table 1
Compilation of recommended values for sticking coefficients for hydrocarbon radicals on a–C:H surfaces

Radical	s	Ref.	Remarks
C	1		
CH	1	[54]	
CH_2	0.025	[55]	Measured in plasma
CH_3	10^{-4}	[13,28]	Surface not activated
CH_3	10^{-2}	[28]	Surface activated, e.g., co-bombardment with H or ions
C_2H	0.80	[13]	Measured in plasma
C_2H_3	0.35	[13]	Measured in plasma
C_2H_5	0.03	[56]	Measured in plasma

The values determined in plasmas are surface loss probabilities and represent an upper limit for s.

600 K and low ion energies) that led to the production of many CH species.

Low-temperature laboratory plasma experiments have shown that net deposition is always a competition between deposition and erosion. It is reasonable to assume that this is also true in fusion devices. This means that deposition occurs at all surfaces which are in line of sight to the source of particle generation and the boundary plasma. But on plasma facing surfaces that are intersecting magnetic field lines the high impinging ion flux causes strong reerosion so that the net deposition decreases and may even change to net erosion. This can, for example, explain the observed torodial asymmetric deposition patterns on the JET divertor tiles reported in [52]. From this we can conclude that the pattern formation of co-deposited layers is significantly influenced, if not dominated, by reerosion. The situation remains, however, rather complicated due to the strong synergistic effects between different types of species. We can assume that most of the deposition close to the main erosion sources in the inner divertor, i.e., the strike zone, is caused by high-sticking species. Only this assumption can explain the steep gradients and the absolute amounts observed experimentally in remote areas of the inner divertor [4–6,11,53]. However, as has been shown in the particle-beam experiments, the sticking coefficient of low-sticking species can be enhanced by up to 2 orders of magnitude if atomic H or ion bombardment activates the surface. This means that at least a part of the observed pattern in remote areas, such as under the divertor structure of ASDEX Upgrade, might be influenced by the parasitic plasma [4,5] which can cause surface activation. If this were to be the case, then deposition of low-sticking species would be just a measure of the surface activation and the deposition profile might be caused by the plasma density profile in front of the surface because the plasma density determines the ion flux density which in turn determines the degree of activation of the surface.

Although much progress has been made in understanding the redeposition process in fusion devices, it is obvious that many open questions remain. These have to be addressed in further experiments in low-temperature laboratory plasmas as well as in fusion devices. Dedicated experiments to determine the particle fluxes to relevant deposition areas in tokamaks would be very helpful to clarify the dominant processes.

References

[1] G. Federici, C.H. Skinner, J.N. Brooks, J.P. Goad, C. Grisolia, A.A. Haasz, A. Hassanein, V. Philipps, C.S. Pitcher, J. Roth, et al., Nucl. Fus. 41 (2001) 1967.

[2] J.P. Goad, N. Bekris, J.D. Elder, S. Erents, D. Hole, K. Lawson, G. Matthews, R. Penzhorn, P. Stangeby, J. Nucl. Mater. 290–293 (2001) 224.

[3] M. Mayer, V. Phillips, P. Wienhold, H. Esser, J. von Seggern, M. Rubel, J. Nucl. Mater. 290–293 (2001) 381.

[4] V. Rohde, M. Mayer, the ASDEX Upgrade Team, J. Nucl. Mater. 313–316 (2003) 337.

[5] V. Rohde, M. Mayer, the ASDEX Upgrade Team, Phys. Scr. T103 (2003) 25.

[6] M. Mayer, V. Rohde, A. von Keudell, the ASDEX Upgrade Team, J. Nucl. Mater. 313–316 (2003) 429.

[7] M. Mayer, V. Rohde, J. Likonen, E. Vainonen-Ahlgren, K. Krieger, X. Gong, J. Chen, ASDEX Upgrade Team, in: Proceedings PSI-16, 2004. doi:10.1016/j.jnucmat.2004.10.046.

[8] M. Rubel, J.P. Goad, P. Wienhold, G. Matthews, V. Phillips, M. Stamp, T. Tanabe, Phys. Scr., in press.

[9] J.P. Goad, P. Andrew, D. Hole, S. Lehto, J. Likonen, G. Matthews, M. Rubel Contributors to the EFDA-JET work programme, J. Nucl. Mater. 313–316 (2003) 419.

[10] M. Rubel, J.P. Goad, N. Bekris, S. Erents, D. Hole, G. Matthews, R. Penzhorn Contributors to the EFDA-JET work programme, J. Nucl. Mater. 313–316 (2003) 321.

[11] M. Mayer, A. von Keudell, V. Rohde, P. Goad, J. contributors, in: R. Koch, S. Lebedev (Eds.), Proceedings of the 30th EPS Conference, European Physical Society, 2003, p. O2.6A.

[12] C. Hopf, K. Letourneur, W. Jacob, T. Schwarz-Selinger, A. von Keudell, Appl. Phys. Lett. 74 (1999) 3800.

[13] C. Hopf, T. Schwarz-Selinger, W. Jacob, A. von Keudell, J. Appl. Phys 87 (2000) 2719.

[14] A. von Keudell, C. Hopf, T. Schwarz-Selinger, W. Jacob, Nucl. Fus. 39 (1999) 1451.

[15] V. Rohde, M. Mayer, J. Likonen, R. Neu, T. Puetterich, E. Vainonen-Ahlgren, the ASDEX Upgrade Team, in: Proceedings PSI-16, 2004. doi:10.1016/j.jnucmat.2004.10.110.

[16] C.H. Skinner, unpublished results, 2004.

[17] von Seggern et al., J. Nucl. Mater. 313–316 (2003) PSI15.

[18] H.-G. Esser et al., in Proceedings PSI-16, 2004. doi:10.1016/j.jnucmat.2004.10.112.

[19] D. Whyte, G. Tynan, R. Doerner, J. Brooks, Nucl. Fus. 41 (2001) 47.

[20] P. Kornejew, W. Bohmeyer, H.-D. Reiner, C.H. Wu, Phys. Scr. T 91 (2001) 29.

[21] I. Arkhipov, W.B. et al., Tech. Rep., EFDA Task, Final Report, 2003.

[22] A. von Keudell, W. Jacob, J. Appl. Phys. 79 (1996) 1092.

[23] W. Jacob, Thin Solid Films 326 (1998) 1.

[24] T. Schwarz-Selinger, A. von Keudell, W. Jacob, J. Appl. Phys. 86 (1999) 3988.

[25] E. Vietzke, K. Flaskamp, V. Phillips, G. Esser, P. Wienhold, J. Winter, J. Nucl. Mater. 145–147 (1987) 443.

[26] E. Vietzke, A.A. Haasz, in: W. Hofer, J. Roth (Eds.), Physical Processes of the Interaction of Fusion Plasmas with Solids, Academic Press, 1996, p. 135.

[27] J. Kiippers, Surf. Sci. Rep. 22 (1995) 249.

[28] M. Meier, A. von Keudell, J. Appl. Phys. 90 (2001) 3585.

[29] W. Jacob, C. Hopf, M. Meier, T. Schwarz-Selinger, in: Interaction of Low-energy Ions and Hydrocarbon Radicals with Carbon Surfaces, Springer, 2004 (Chapter. 3.3).

[30] A. von Keudell, W. Jacob, Prog. Surf. Sci., in press.

[31] A.A. Haasz, J.W. Davis, Phys. Scr. in press.
[32] J.W. Davis, A.A. Haasz, P.C. Stangeby, J. Nucl. Mater. 155–157 (1988) 234.
[33] E. Vietzke, K. Flaskamp, V. Philipps, J. Nucl. Mater. 111&112 (1982) 763.
[34] C. Hopf, A. von Keudell, W. Jacob, J. Appl. Phys. 94 (2003) 2373.
[35] A. von Keudell, T. Schwarz-Selinger, W. Jacob, J. Appl. Phys. 89 (2001) 2979.
[36] M. Meier, R. Preuss, V. Dose, New J. Phys. 5 (2003) 133.1.
[37] P. Träskelin, E. Salonen, K. Nordlund, A. Krasheninnikov, J. Keinonen, C. Wu, J. Appl. Phys. 93 (2003) 1826.
[38] P. Träskelin, E. Salonen, K. Nordlund, J. Keinonen, C.H. Wu, J. Nucl. Mater. 334 (2004) 65.
[39] C. Hopf, A. von Keudell, W. Jacob, Diamond Relat. Mater. 12 (2003) 85.
[40] C. Hopf, A. von Keudell, W. Jacob, J. Appl. Phys. 93 (2003) 3352.
[41] C. Hopf, PhD thesis, Universitat Bayreuth, 2003.
[42] W. Möller, B.M.U. Scherzer, Appl. Phys. Lett. 50 (1987) 1870.
[43] T. Zecho, B.D. Brandner, J. Biener, J. Kiippers, J. Phys. Chem. B 105 (2001) 6194.
[44] T. Zecho, B.D. Brandner, J. Biener, J. Kiippers, J. Phys. Chem. B 106 (2002) 610.
[45] W. Jacob, C. Hopf, A. von Keudell, T. Schwarz-Selinger, in: Hydrogen Recycling at Plasma Facing Materials, Kluwer Academic, 2000, p. 331.
[46] B.V. Mech, A.A. Haasz, J.W. Davis, J. Appl. Phys. 84 (1998) 1655.
[47] B.V. Mech, A.A. Haasz, J.W. Davis, J. Nucl. Mater. 255 (1998) 153.
[48] E. Vietzke, V. Phillips, K. Flaskamp, C. Wild, in: P. Koidl, P. Oelhafen (Eds.), E-MRS Proceedings XVII, Les Edition de Physique, 1987, p. 351.
[49] U. Fantz, H. Paulin, Phys. Scr. T 91 (2001) 25.
[50] R. Pugno, A. Kallenbach, J. Likonen, E. Vainonen-Ahlgren, D. Coster, R. Dux, A. Kirschner, K. Krieger, V. Rohde, U. Fantz, et al., in: Proceedings PSI-16, 2004, p. PI-34. doi:10.1016/j.jnucmat.2004.09.053.
[51] S. Brezinsek, in: Proceedings PSI-16, 2004. doi:10.1016/j.jnucmat.2004.10.114.
[52] K. Sugiyama, K. Miyasaka, T. Tanabe, M. Glugla, N. Bekris, J.P. Goad, J. Nucl. Mater. 313–316 (2003) 507.
[53] M. Mayer, V. Rohde, T. Puetterich, P. Goad, P. Wienhold, JET-EFDA Contributors, ASDEX Upgrade Team, Phys. Scr., in press.
[54] M. Bauer, PhD thesis, Universitat Bayreuth, 2004.
[55] H. Kojima, H. Toyoda, H. Sugai, Appl. Phys. Lett. 55 (1989) 1507.
[56] J. Perrin, M. Shiratani, P. Kae-Nune, H. Videlot, J. Jolly, J. Guillon, J. Vac. Sci. Technol. A 16 (1998) 278.